JOURNAL OF FORENSIC SCIENCES

J Forensic Sci, September 2012, Vol. 57, No. 5
doi: 10.1111/j.1556-4029.2012.02075.x
Available online at: onlinelibrary.wiley.com

TECHNICAL NOTE

PHYSICAL ANTHROPOLOGY

Pierre Guyomarc'h,[1] *M.Sc.; Bruno Dutailly,*[1] *M.Sc.; Christine Couture,*[1] *Ph.D.; and Hélène Coqueugniot,*[1] *Ph.D.*

Anatomical Placement of the Human Eyeball in the Orbit—Validation Using CT Scans of Living Adults and Prediction for Facial Approximation*

ABSTRACT: Accuracy of forensic facial approximation and superimposition techniques relies on the knowledge of anatomical correlations between soft and hard tissues. Recent studies by Stephan and collaborators (6,8,10) reviewed traditional guidelines leading to a wrong placement of the eyeball in the orbit. As those statements are based on a small cadaver sample, we propose a validation of these findings on a large database (n = 375) of living people. Computed tomography scans of known age and sex subjects were used to collect landmarks on three-dimensional surfaces and DICOM with TIVMI. Results confirmed a more superior and lateral position of the eyeball relatively to the orbital rims. Orbital height and breadth were used to compute regression formulae and proportional placement using percentages to find the most probable position of the eyeball in the orbit. A size-related sexual dimorphism was present but did not impact on the prediction accuracy.

KEYWORDS: forensic science, facial reconstruction, facial reproduction, computed tomography, Oculus, TIVMI

Methods of craniofacial identification, such as facial approximation or superimposition, require accurate and reliable guidelines based on large databases (1,2). Facial recognition is a complex process that relies on several factors, of which the shape and the proportion of the facial organs are some of the most important (3,4). The placement of the eyeball tends to influence the positioning of the canthi in manual reconstruction (5); any error in the first will lead to errors in the second. For facial approximation, the traditional guidelines for such placement have been recently discussed. See Stephan and Davidson (6) for an exhaustive review of those guidelines. Up to the reevaluation of the rules, the eyeball was advised to be placed centrally in the orbit and its projection to be tangent to a line joining the superior and inferior orbital rims (7). Those rules have been rejected as inaccurate after a review of the exophthalmometry literature (8), through a magnetic resonance imaging (MRI) sample (9) and by cadaver-based studies (6,10). The latter study is based on a small elderly cadaver sample (n = 13). Even if the comparability of those results with living persons has been hypothesized, such application can be criticized. This paper follows a preliminary study (11) and presents similar data obtained through computed tomography (CT) from a large database of living subjects. The goals are to validate previous observations, to measure age and sex influences and asymmetry, and to propose a reproducible method of eyeball positioning in the orbit.

[1]Université Bordeaux 1, UMR 5199 - PACEA, Anthropologie des Populations Passées et Présentes (A3P), Avenue des Facultés, Bâtiment B8, 33405 Talence Cedex, France.

*Financial support for this work has been provided by a PhD scholarship granted by the French Ministry of Research (Ministére de l'Enseignement Supérieur et de la Recherche), and a BQR (Bonus Qualité Recherche "Reconstitution faciale par imagerie 3D", Université Bordeaux 1).

Received 1 Mar. 2011; and in revised form 4 May 2011; accepted 15 May 2011.

Material and Methods

Nine hundred CT scans were collected in French hospitals with radiologists in accordance with ethical committee guidelines. After excluding subjects showing any pathological or traumatic effects and selecting only high-resolution scans, the study sample contained 375 adult individuals of known age and sex. The sex ratio was 1:0.84 (204 men and 171 women), and the mean age was 52.2 years (min = 18; max = 95; σ = 20.3). There was no significant difference in the age distribution between sex according to a t-test (t = −0.09; p = 0.92). Ethnicity information was not available because of French ethical issues, but the sample is assumed to be proportional to the present diversity of the French population.

The CT scans were processed with TIVMI (Treatment and Increased Vision for Medical Imaging; http://www.pacea.u-bordeaux1.fr/TIVMI/), developed by one of the authors (BD). This computer program has been designed for morphometrics and anthropological research. It facilitates basic geometric operations and accurate surface reconstructions so that the craniofacial morphology can be measured objectively. After importing the DICOM files (Digital Imaging and Communications in Medicine), the superior part of the skull was reconstructed using an algorithm based on the half-maximum height (HMH) protocol in three dimensions (3D) (12). This technique detects the best limit between materials of different densities (between the bone and the soft tissues in our case) without any subjective intervention of the user (13). The reconstructed cranium in 3D is then used to position the bony landmarks *nasion*, *orbitale,* and *porion* (Table 1). The Frankfurt Horizontal (FH) plane is created based on both the right and the left *porion* and on both the right and the left *orbitale*, according to its original definition (14,15) by computing mean planes (Fig. 1). The FH plane is thus used to define the orthogonal frontal and sagittal

TABLE 1—*Landmarks used in this study.*

Landmark	Definition
Porion* (po)	The highest point on the superior margin of the external auditory meatus
Orbitale* (or)	The lowest point on the orbital rim
Nasion* (n)	The junction of the internasal suture with the nasofrontal suture
Dacryon* (d)	The junction of the sutures between the frontal, maxillary, and lacrimal bones
Ectoconchion* (ek)	The most lateral point of the orbital rim following a line bisecting the orbit from the dacryon
Supraconchion* (sk)	The highest point on the orbital rim
Frontomalare orbitale* (fmo)	The point on the orbital rim at the junction of the sutures between the frontal and zygomatic bones
Deepest point of the lateral orbital margin** (dlom)	The deepest point on the lateral orbital rim
Oculus anterius (oa)	The most anterior point of the eyeball
Oculus posterius (op)	The most posterior point of the eyeball
Oculus superius (os)	The most superior point of the eyeball
Oculus inferius (oi)	The most inferior point of the eyeball
Oculus mediale (om)	The most medial point of the eyeball
Oculus laterale (ol)	The most lateral point of the eyeball

*From (16), **from (6).

planes. The landmarks of the orbit can be positioned with reproducibility using those reference planes (Table 1).

Because the eyeball does not display a density different enough from the other soft tissues, it is not possible to reconstruct it accurately in 3D. Landmarks on the eyeball are recorded directly on the DICOM files. To avoid an orientation bias, the original files were resliced according to the FH and sagittal planes. This procedure allowed the most anterior (oa; homologous to the *pupulare*, center of the pupil) and posterior (op) points of the eyeball to be positioned on the same slice, preserving a reproducible orientation independent of the patient's gaze (Fig. 1).

Repeated measurements were performed by a student not involved in the study, on 10 subjects. In parallel, one of the authors (PG) made the same measurements three times on five subjects. The mean dispersion of each landmark was calculated by computing the distance between the repeated measures. The mean intra-observer variability was systematically below 1 mm for all landmarks. As expected, the mean inter-observer dispersion was higher but remains below 2 mm.

The interlandmark distances between the two points a and b in 3D (x, y, z) were extracted with the Pythagorean formula: $\mathrm{Dist}_{(a\text{-}b)} = \sqrt{((x_a-x_b)^2+(y_a-y_b)^2+(z_a-z_b)^2)}$. Because the eyeball cannot be strictly considered a sphere, its volume (v) was calculated as an ellipsoid. The radius of the eyeball in the three planes was labeled a, b, and c: $v = (4/3)\pi abc$. The extracted measurements (6,10,16) are listed in Table 2.

The measurements recorded in projection, such as the orbital height or the distances from the most anterior point of the eyeball and the orbital rims, were made by orthogonal projection of the landmarks on the reference planes in TIVMI. Statistical analyses were performed with Statistica® (v7.1; Statsoft®, Tulsa, OK). The Student's *t*-test was used to check the symmetry between the right and left variables and to evaluate sexual dimorphism. Pearson's correlation was used to explore the influence of age on the orbital morphology. A Bonferroni adjustment was applied to the *p*-level for the *t*-tests to avoid type 1 errors (17). Linear regressions were used to propose formulae predicting the eyeball positioning in the orbit.

Results

All variables follow a normal distribution according to a Shapiro–Wilk test, except the eyeball volume, which was relatively constant across individuals (nonparametric tests were thus used to study this variable). Table 3 presents the descriptive statistics of the orbit and eyeball metrics, along with the results of the tests concerning asymmetry, sexual dimorphism, and age influence.

A significant asymmetry was detected in the orbital breadth, the right orbit being wider. The slight asymmetry in the distance between the eyeball and the medial orbital margin could not

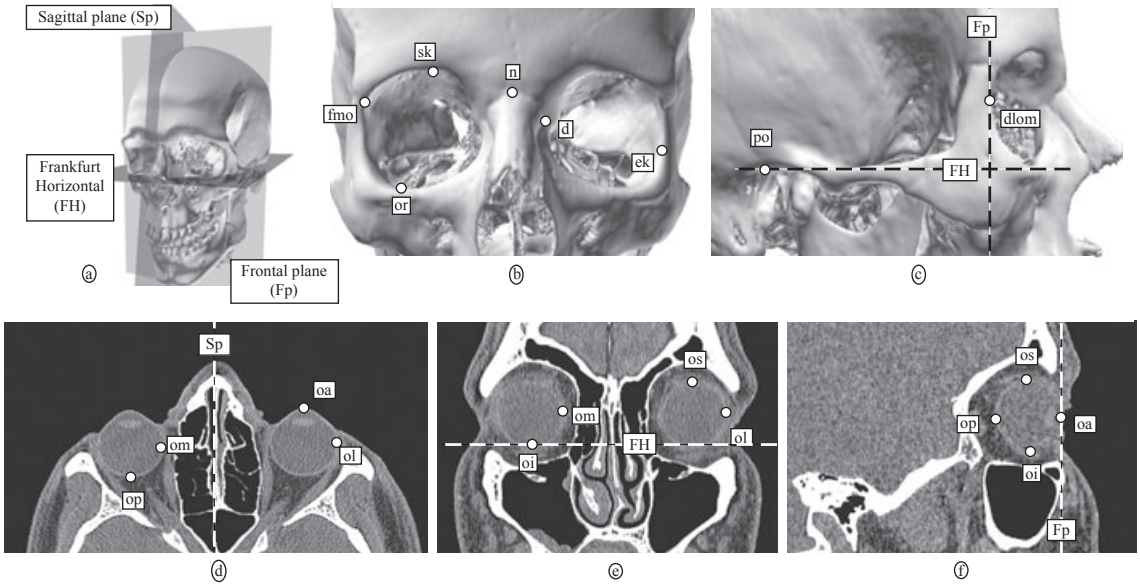

FIG. 1—*Landmarks and planes on bone reconstruction (a: position of the reference planes; b: frontal view; c: lateral view) and on DICOM files (d: superior view; e: frontal view; f: lateral view).*

TABLE 2—*Measurements used in this study.*

Measurement	Definition
Orbital height (OBH)*	Projected vertical distance between sk and or
Orbital breadth (OBB)*	Direct distance between ek and d, bisecting the orbit
Eyeball projection**	Projected distance between dlom and oa
Superior orbital margin (SOM)—oa**	Projected vertical distance between oa and sk
Inferior orbital margin (IOM)—oa**	Projected vertical distance between oa and or
Lateral orbital margin (LOM)—oa**	Projected horizontal distance between oa and ek
Medial orbital margin (MOM)—oa**	Projected horizontal distance between oa and d
Eyeball volume	Calculated from the three diameters of the eyeball

*From (16), **from (6).

be considered significant after a Bonferroni adjustment (p-level = 0.006). All of the measurements were smaller in women, but the sexual dimorphism was significant for orbital breadth, eyeball projection, and mediolateral positioning. A Bonferroni correction rejected the significant sex influence on the eyeball position regarding the inferior orbital rim and on the right orbital height (p-level = 0.003). Age influence was negligible ($r < 0.22$) in all hard and soft tissues dimensions. Univariate analyses of covariance (ANCOVA) using age and sex did neither allow a better understanding of the relationship between those factors in the variables nor reveal sex-specific pattern.

The eyeball volume was relatively constant. This variable did not present any strong correlation ($r < 0.25$) with the orbital height or breadth. The mean anteroposterior diameter was 23.7 mm, the mean mediolateral diameter was 24.3 mm, and the mean superoinferior diameter was 24.6 mm. Even if the volume was significantly larger in men, the millimeter difference (<0.5 mm in diameter) will be negligible between the sexes when performing a facial approximation or superimposition.

The sexual dimorphism in eyeball position (in the mediolateral plane) is likely size related. To define a strict relationship between orbital shape and eyeball position, the relative distances of the eyeball to the medial, superior, and lateral (for anterior projection) margins were converted to percentages of orbital breadth (OBB) and height (OBH), respectively. Eyeball projection is also well correlated to orbital height; this bony measurement was thus chosen to predict the projection. The distance from the oculus anterius to the most superior part of the orbit (SOM) averaged 44.1% of the OBH (min = 34.3%; max = 55.3%; SD = 3.9%). The mediolateral position of the eyeball, measured from the dacryon (MOM), averaged 57.6% of the OBB (min = 48.1%; max = 69.5%; SD = 3.4%). The projection of the eyeball from the deepest point of the lateral orbital margin (dLOM) averaged 51.3% of the orbital height (min = 34.2%; max = 70.5%; SD = 6.3%). These results, based on both the right and left orbits, are presented in Fig. 2.

The different bony measurements recorded in this study were evaluated in terms of their correlation with the eyeball positioning (systematically according to the oculus anterius). Simple regressions were sufficiently reliable to estimate the position of the eyeball in the mediolateral and superoinferior planes according to the medial and superior orbital margins, respectively. Concerning the eyeball projection, no single variable showed a sufficient correlation to aid the prediction. Nevertheless, a multiple regression produced an acceptable prediction equation using the orbital height and the distance from the nasion to the frontomalare orbitale. The standard error of the estimate (SEE) was slightly lower than the standard deviation of the measurements: the prediction formulae should thus be preferred to the simple application of means. Sex-specific

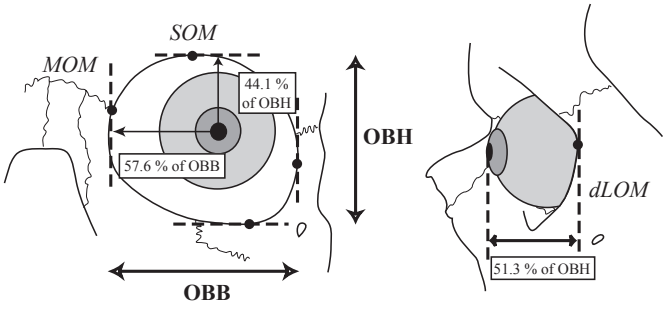

FIG. 2—*Proportional placement of the eyeball using the medial (MOM), superior (SOM), and deepest point of the lateral (dLOM) orbital margins with the percentages of the orbital height (OBH) and breadth (OBB).*

TABLE 3—*Descriptive statistics (mean, minimum, maximum, standard deviation), asymmetry, sexual dimorphism, and age influence on the orbital and the right (R) and left (L) eyeball measurements for males (M) and females (F).*

		Mean	Mean (M)	Mean (F)	Min	Max	SD	Asym	Sex	Age
Measurement	Side			*(mm)*				*(p)*	*(p)*	*(r)*
Orbital height (OBH)	R	35.7	35.9	35.4	29.0	44.1	2.55	0.80	0.04*	0.22
	L	35.6	35.8	35.4	28.4	45.6	2.45		0.08	0.17
Orbital breadth (OBB)	R	39.2	40.0	38.3	33.0	45.3	1.93	0.00**	0.00**	0.17
	L	38.7	39.5	37.8	33.2	45.6	1.89		0.00**	0.08
Eyeball projection	R	18.3	18.9	17.7	12.3	25.1	2.33	0.43	0.00**	0.13
	L	18.2	18.7	17.6	12.6	25.6	2.32		0.00**	0.07
SOM—oa	R	15.7	15.7	15.7	11.3	21.1	1.93	0.20	0.87	0.11
	L	15.9	16.0	15.7	11.0	22.9	1.91		0.29	0.08
IOM—oa	R	20.0	20.3	19.7	14.7	25.1	1.85	0.08	0.01*	0.18
	L	19.8	19.9	19.7	15.3	25.0	1.72		0.20	0.14
LOM—oa	R	16.6	16.8	16.3	12.1	20.7	1.47	0.21	0.00**	0.16
	L	16.4	16.7	16.1	11.0	20.5	1.62		0.00**	−0.07
MOM—oa	R	22.6	23.2	21.9	18.7	27.5	1.67	0.01*	0.00**	0.05
	L	22.3	22.8	21.7	17.6	28.1	1.81		0.00**	0.15
Eyeball volume (mm^3)	R	7439.1	7643.7	7195.1	4682.9	11450.4	891.92	0.78	0.00**	−0.13
	L	7457.5	7662.0	7213.6	4972.6	12654.6	893.93		0.00**	0.15

Statistically significant *$p < 0.05$, **$p < 0.001$.

TABLE 4—*Prediction formulae and percentages for proportional placement of the eyeball in the orbit, along with the respective errors.*

	Prediction Through Regression			Prediction by Proportionality	
Eyeball Position	Formulae	r^2	*SEE* (mm)	Percentage	*SEE* (mm)
Superoinferior	0.54*OBH—3.5	0.49	1.4	44.1% of OBH from sk	1.4
Mediolateral	0.59*OBB—0.4	0.42	1.3	57.6% of OBB from d	1.3
Anteroposterior	0.23*OBH + 0.26*n-fmo—3.38	0.20	2.1	51.3% of OBH from dlom	2.3

regressions did not enhance the prediction of the eyeball position in the orbit.

The mean percentages of the orbital height and breadth have also been applied to predict the position of the eyeball in the three planes. The resulting SEE is similar to the one resulting from the prediction formulae. Table 4 summarizes those results based on both the right and left orbits.

Discussion and Conclusion

The more superolateral position of the eyeball in the orbit has been confirmed through the measurement of 375 individuals. These results agree with the preliminary statements made in a previous study based on 140 subjects (11), and they confirm the cadaver-based studies (6,10). The stability of the eyeball volume is also consistent with MRI-based clinical recent observations (18–20). Our large sample made it possible to statistically explore the orbit and eyeball morphology with regard to sexual dimorphism and age influence. Only sex influences the orbital breadth and the projection of the eyeball; this is potentially linked with the shape of the male lateral orbital rim because the measurement of the projection depends on this margin. The use of percentages or formulae eliminates the need to include size-related sexual dimorphism in the prediction. Because the sample is cross-sectional, the age influence can also be interpreted as secular trends, but the variables studied did not produce significant results.

The functional matrix of the orbital region (soft and hard tissues participating in the vision) is common to all human subjects (21). The differential sexual dimorphism between orbital height and breadth has been observed in other samples (22). Because each orbital matrix is part of the facial matrix, this phenomenon cannot be attributed solely to the influence of the organs of vision or the orbicular muscle activity. A broader pattern including other factors (the biomechanics of the cranial vault and mastication, ontogeny, etc.) should be considered (23).

In terms of methodology, rather than relying on empirical distances, the placement of the eyeball can thus be done based on the specific morphology of each subject, with no regard to age or sex. Our sample is wide and homogeneous; our results validated previous published findings. We hypothesize that the methods described here are applicable. These guidelines can be used for manual or computer-based facial approximation and superimposition in two or three dimensions. Moreover, this study emphasizes the critical importance of reassessing and reevaluating the traditional rules used in craniofacial identification.

Acknowledgments

The authors wish to thank all of the health care professionals who contributed to the CT scan collection: Dr. Jean-Yves Tanguy and Pr. Christophe Aubé (CHU Angers); Pr. Christophe Cognard, Serge Martinez, and Corinne Viard (Hôpital Purpan, Toulouse); Dr. Paul Ardilouze, Dr. David Higué, and Dr. Charles Laurent (CHCB, Bayonne); Dr. Jack Richecoeur (CH René Dubos, Pontoise); Dr. Raphaël Legghe (Polyclinique du Bois, Lille); Pr. Jean-Nicolas Dacher and Dr. Emmanuel Gerardin (CHU Rouen); Dr. Anne-Sophie Ricard and Pr. Vincent Dousset (CHU Pellegrin Tripode, Bordeaux); Pr. Michel Montaudon (Hôpital Haut-Lévêque, Pessac); Dr. Jean-Paul Delhaye (CH Pierre Ourdot, Bourgoin-Jallieu). We are also grateful to Léonie Rey (Université Bordeaux 1) for the replicate measurements she performed and to Frédéric Santos for the statistical advice he provided.

References

1. Claes P, Vandermeulen D, De Greef S, Willems G, Clement JG, Suetens P. Computerized craniofacial reconstruction: conceptual framework and review. Forensic Sci Int 2010;201(1–3):138–45.
2. Stephan CN. The human masseter muscle and its biological correlates: a review of published data pertinent to face prediction. Forensic Sci Int 2010;201(1–3):153–9.
3. Haig ND. The effect of feature displacement on face recognition. Perception 1984;13(5):505–12.
4. Smeets D, Claes P, Vandermeulen D, Clement JG. Objective 3D face recognition: evolution, approaches and challenges. Forensic Sci Int 2010;201(1–3):125–32.
5. Wilkinson CM. Forensic facial reconstruction. Cambridge, UK: Cambridge University Press, 2004.
6. Stephan CN, Davidson PL. The placement of the human eyeball and canthi in craniofacial identification. J Forensic Sci 2008;53(3):612–9.
7. Taylor KT. Forensic art and illustration. Boca Raton, FL: CRC Press, 2001.
8. Stephan CN. Facial approximation: globe projection guideline falsified by exophtalmometry literature. J Forensic Sci 2002;47(4):730–5.
9. Wilkinson CM, Mautner SA. Measurement of eyeball protrusion and its application in facial reconstruction. J Forensic Sci 2003;48(1):12–6.
10. Stephan CN, Huang AJR, Davidson PL. Further evidence on the anatomical placement of the human eyeball for facial approximation and craniofacial superimposition. J Forensic Sci 2009;54(2):267–9.
11. Guyomarc'h P, Coqueugniot H, Dutailly B, Couture C. Anatomical placement of the human eyeball in the orbit—new metric data and guidelines proposal for facial identification. Am J Phys Anthropol 2010;141(S50):120.
12. Dutailly B, Coqueugniot H, Desbarats P, Gueorguieva S, Synave R. 3D surface reconstruction using HMH algorithm. Proc IEEE Int Conf Image Proc (ICIP09) 2009;2505–8.
13. Spoor CF, Zonneveld FW, Macho GA. Linear measurements of cortical bone and dental enamel by computed tomography: applications and problems. Am J Phys Anthropol 1993;91(4):469–84.
14. Hrdlicka A. Anthropometry. Am J Phys Anthropol 1919;2(4):401–28.
15. Seal WM. The relationship of the Frankfort Horizontal to the His line. Angle Orthod 1964;34(4):235–43.
16. Bräuer G. Osteometrie. In: Knussmann R, Martin R, editors. Anthropologie Handbuch der vergleichenden Biologie des Menschen. Stuttgart, New York: Fisher, 1988;160–231.
17. Abdi H. The Bonferroni and Sidak corrections for multiple comparisons. In: Salkind N, editor. Encyclopedia of measurement and statistics. Thousand Oaks, CA: Sage, 2007;103–7.

18. Furuta M. Measurement of orbital volume by computed tomography: especially on the growth of the orbit. Jpn J Ophthalmol 2001;45(6):600–6.
19. Detorakis ET, Drakonaki E, Papadaki E, Tsilimbaris MK, Pallikaris IG. Evaluation of globe position within the orbit: clinical and imaging correlations. Br J Ophthalmol 2010;94(1):135–6.
20. Detorakis ET, Drakonaki E, Papadaki E, Pallikaris IG, Tsilimbaris MK. Effective orbital volume and eyeball position: an MRI study. Orbit 2010;29(5):244–9.
21. Moss ML, Young RW. A functional approach to craniology. Am J Phys Anthropol 1960;18(4):281–92.
22. Ji Y, Qian Y, Dong Y, Zhou H, Fan X. Quantitative morphometry of the orbit in Chinese adults based on a three-dimensional reconstruction method. J Anat 2010;217(5):501–6.
23. Urbanova P. A study of human craniofacial variation by using geometric morphometrics. Brno, Czech Republic: Masaryk University, 2009.

Additional information and reprint requests:
Pierre Guyomarc'h, M.Sc.
Université Bordeaux 1
UMR 5199 - PACEA
Anthropologie des Populations Passées et Présentes (A3P)
Avenue des Facultés
Bâtiment B8
33405 Talence Cedex
France
E-mail: pierreguyo@gmail.com